Technologies **2015**, *3*, 47-57; doi:10.3390/technologies3010047

OPEN ACCESS

technologies

ISSN 2227-7080

www.mdpi.com/journal/technologies

Article

Comparison of Grain Structure, Electrical and Magnetic Properties of $BaTiO_3$ and $Ni_{0.5}Zn_{0.5}Fe_2O_4$ Ceramics Sintered Using Microwave and Conventional Techniques

Santiranjan Shannigrahi * and Chee Kiang Ivan Tan

Institute of Materials Research and Engineering, Agency for Science Technology and Research (A*STAR), 3 Research Link, Singapore 117602, Singapore; E-Mail: ivan-tan@imre.a-star.edu.sg

* Author to whom correspondence should be addressed; E-Mail: santi-s@imre.a-star.edu.sg; Tel.: +65-6874-8299; Fax: +65-6872-0785.

Academic Editor: Manoj Gupta

Received: 4 January 2015 / Accepted: 10 March 2015 / Published: 17 March 2015

Abstract: $BaTiO_3$ (BT) and $Ni_{0.5}Zn_{0.5}Fe_2O_4$ (NZF) ceramic disc specimens were prepared using commercial grade powders sintering by conventional (CV) and microwave (MW) sintering techniques. In both the sintering techniques the set sintering temperatures were in the range of 850 °C to 1000 °C and time from 0.5 to 2 h. Structure, microstructure, dielectric, ferroelectric and magnetic properties have been compared for the as sintered BT and NZF ceramic specimens. Comparatively large grain size and higher density observed for the samples sintered at same temperature and shorter holding time using microwave. Magnetic properties of the NZF samples sintered using MW at a temperature of 950 °C show a higher saturation magnetization (M_s) value of 88 emu/g.

Keywords: microwave sintering; ferrites; dielectric; ferroelectric; magnetic; XRD

1. Introduction

The grain growth in polycrystalline ceramics during sintering process of powders is an extremely important phenomenon. Many different properties of ceramics depend on the final grain size of the ceramic body. In this regard, $BaTiO_3$ (BT) is being chosen as it has several important functional properties in addition to its lead free nature. BT is stable under high temperatures in various applications like capacitors. Especially multilayer ceramic capacitors (MLCC) based on BT are one of the most important electronic components in surface mounted electronic circuits *etc.* [1–4]. Similarly, $NiZnFe_2O_4$ (NZF) is also one of the technologically important ferrites and found very useful in high frequency applications, as well as its microwave absorption properties [5] because of its high resistivity and low eddy current losses [6–9]. Moreover, BT and NZF are being studied as the multiferroic ceramic composites too [10]. While BT and NZF ceramics are well studied, they are still a topic of active research in order to further enhance or optimize their properties. Most of the useful properties of BT and NZF ceramics are governed by their grain size, so control of homogeneous grain growth at reduced temperatures will be quite useful for the scientific community as well as industry. This work attempts to compare the grain growth of commercial BT and NZF powders heat treated by conventional and microwave techniques in the temperature range of 850 °C–1000 °C and time 0.5 to 2 h. We have also tested the effect of LiF as flux and its effect on the microstructures.

2. Experimental Procedure

Commercial nano powders of BT and NZF ceramics were used as starting materials. Commercial LiF with 2 wt% was added as flux to BT followed by adding ethanol followed by overnight oven drying at 80 °C. All pellets were formed under similar conditions with 1 g of BT or BT + LiF or NZF powders mixed with a binder (Polyethene Glycol) in a mixing bowl. The individual mixtures were compressed into 10 mm diameter pellets by applying a pressure of 10 MPa, followed by overnight oven drying at 80 °C. The BT + LiF and NZF samples were sintered at temperatures of 850, 900, 950 and 1000 °C for 2 h and 30 min under air ambient conditions using conventional and microwave furnaces, respectively as shown in Figure 1a,b below.

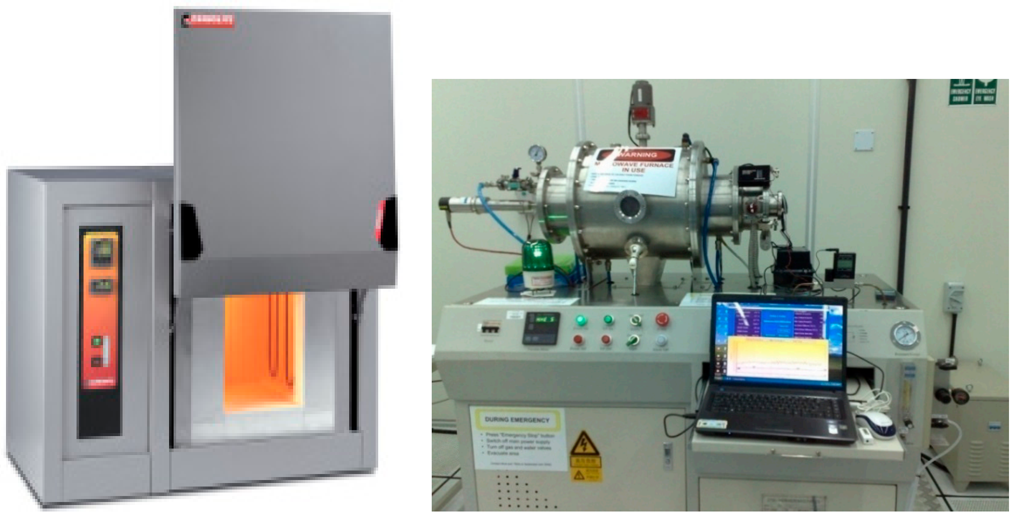

(a) **(b)**

Figure 1. (**a**) Conventional furnace; (**b**) Microwave furnace.

The microwave furnace used was multimode with operation frequency of 2.45 GHz. It was reported earlier [11] that addition a 0.5–3 wt% of LiF flux allowed BT to densify at a temperature much lower than that normally required of pure BT. The crystalline quality of the sintered pellets was analyzed by X-ray diffraction (XRD) analysis and scanning electron microscope (SEM). Atomic force microscope (AFM) was used to statistically estimate the porosity in the sintered ceramics through surface topography analysis. A thin layer of silver paste was applied to both polished surfaces of the sintered BT and NZF samples for measuring their electrical properties. Impedance analyzer (HP, 4194A, Santa Rosa, CA, USA) and ferroelectric testing system (Radiant Technology, Inc. RT66A, Alpharetta, GA, USA) were used to measure the dielectric and ferroelectric properties, respectively. The magnetic properties of the NZF samples were measured using the Physical Property Measurement System (PPMS; Quantum Design, San Diego, CA, USA).

3. Results and Discussion

The crystalline quality of all the BT and NZF ceramics sintered using MW and CV processes in the 850–1000 °C are analyzed. For the sake of simplification and close comparison purposes, the results are presented for the samples sintered at the 900 and 1000 °C temperature for 2 h using CV and 0.5 h using MW process, as these two recipes produced most reasonable results. Results for the specimens sintered at other temperatures are presented where applicable. Figures 2 and 3 depict the XRD spectra of the BT and NZF sintered specimens. No evidence of unwanted phase formation has been found, which indicates that there is no loss of stoichiometry in these ceramics; *i.e.* they remain phase pure single phase [4,6]. However, sharper peaks observed for the MW sintered samples indicate bigger grain sizes compared to CV sintered BT samples. All of the characterized peaks are marked with the standard JCPDS card no. 05-0626 and 019-0629 respectively for BT and NZF ceramics specimens.

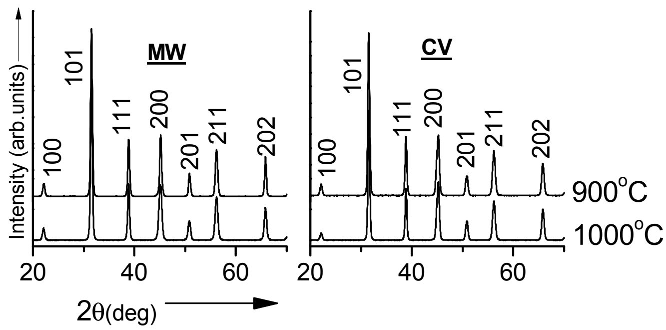

Figure 2. XRD patterns of conventional (CV) and microwave (MW) sintered $BaTiO_3$ (BT) ceramics.

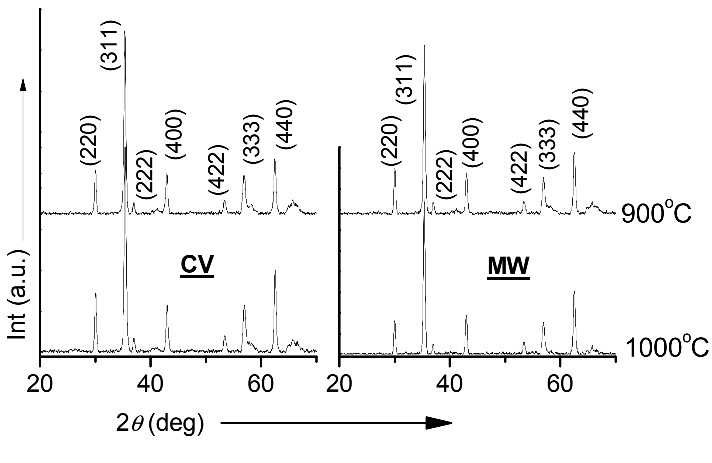

Figure 3. XRD patterns of CV and MW sintered $Ni_{0.5}Zn_{0.5}Fe_2O_4$ (NZF) ceramics.

We measured the shrinkage of the sintered samples. Figure 4 shows the pictures of the NZF ceramics before and after sintering. The average shrinkage for BT ceramics sintered using CV and MW method is in the range of 5%–7% [12]. Noticeable shrinkage was observed for NZF ceramics, 9%–11% using CV processing and 12%–15% that for MW sintered samples. The maximum shrinkage of 15.45% was observed for NZF ceramics sintered at 950 °C using MW.

Figure 4. Sintered (left) and pre-sintered samples (right).

Microstructures of sintered BT and BT + LiF are shown in Figures 5 and 6. No considerable grain growth is observed up to a sintering temperature of 1000 °C for pure BT. The pure BT ceramics could be still in the initial sintering stage, henceforth the grain sizes are still small. However, the average grain size that of the BT + LiF sample sintered using MW at 900 °C for 0.5 h is ~3.1 µm, which is approximately 2 times larger than the BT + LiF samples sintered using CV at 900 °C for 2 h with average grain size ~1.7 µm. It can be observed that there is a trend of increased grain growth size as the MW sintering temperature increases from 850 °C to 1000 °C. The average grain size values of MW sintered samples are also approximately two times larger than CV sintered samples at the same temperature. Grain sizes for MW sintered NZF at 900 °C are nearly twice that of CV sintered samples (Figure 7). As seen from the results, the microwave sintered samples reach the intermediate or final stage of the sintering process much earlier under the impact of the MW field as compared to CV sintered samples. The highest average grain size of ~1.2 µm is measured for MW sinter samples at 1000 °C and the lowest grain size of 1 µm is measured for CV sinter samples at 900 °C. These results can be backed up from the XRD scans as stated earlier.

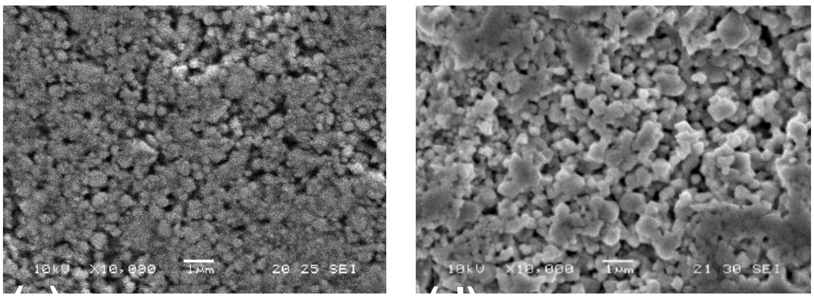

(**a**) (**b**)

Figure 5. *Cont.*

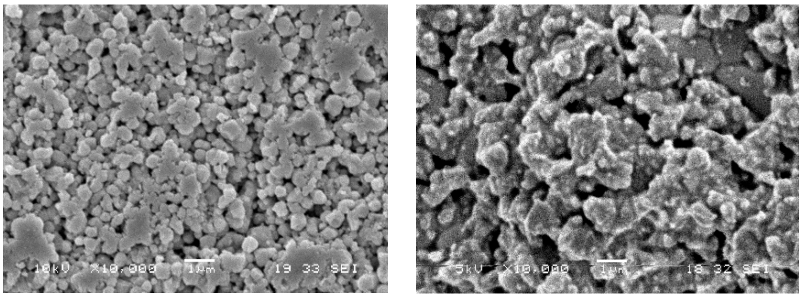

(**c**) (**d**)

Figure 5. SEM morphologies of (**a**) BT-CV-900 °C for 2 h, (**b**) BT-CV-1000 °C for 2 h, (**c**) BT-MW-900 °C for 0.5 h, (**d**) BT-MW-1000 °C for 0.5 h.

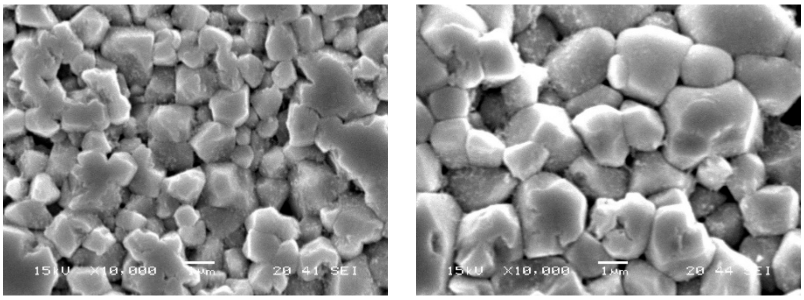

(a) **(b)**

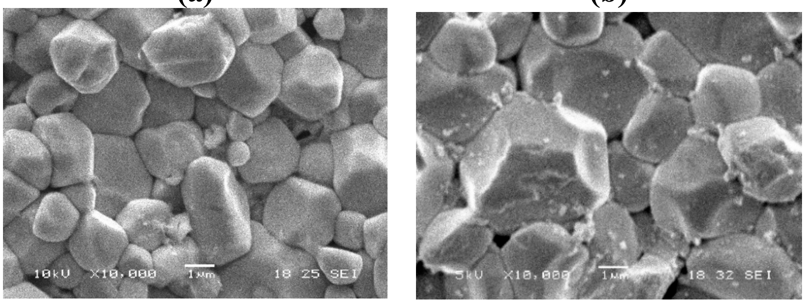

(c) **(d)**

Figure 6. Surface morphologies of (**a**) BT+LiF-CV-900 °C for 2 h, (**b**) BT+LiF-CV-1000 °C for 2 h, (**c**) BT+LiF-MW-900 °C for 0.5 h, (**d**) BT-LiF-MW-1000 °C for 0.5 h.

Sintering of crystalline materials occurred by several mechanisms such as atomic transport, vapor transport (evaporation/condensation), surface diffusion, lattice (volume) diffusion, grain boundary diffusion, and dislocation motion. Figure 8 shows a schematic representation of the matter transport paths for four sintering particles. In conventional heating process, vapor transport, surface diffusion, and lattice diffusion from the particle surfaces to the neck lead to neck growth and coarsening of the particles without densification. The densification mechanism leads through grain boundary diffusion and lattice diffusion from the grain boundary to the neck [13]. In microwave heating, the specimen gets heated from inside to outside just opposite to conventional heating. Moreover, the microwave absorption mainly depends upon the complex permittivity and permeability of the specimens. As both the specimens already develop dipole, so, they responded well to microwave, and resulted good densification in the samples at a short sintering period.

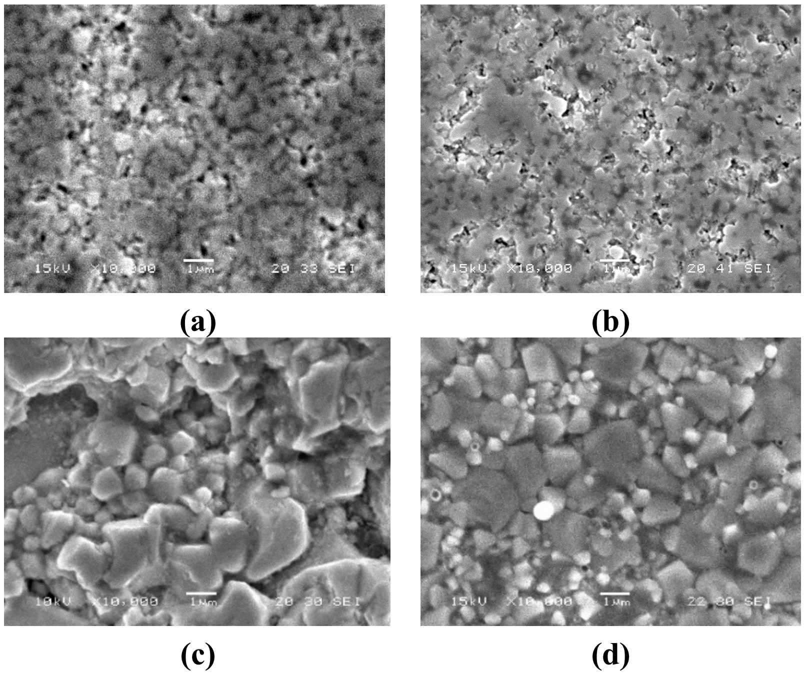

Figure 7. Surface morphologies of (**a**) NZF-CV-900 °C for 2 h, (**b**) NZF-CV-1000 °C for 2 h, (**c**) NZF-MW-900 °C for 0.5 h, (**d**) NZF-MW-1000 °C for 0.5 h.

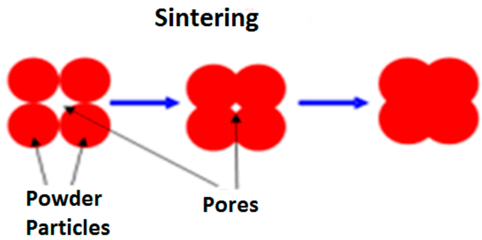

Figure 8. Schematic representation of sintering mechanisms for a system of four particles.

The variation of dielectric constant (*ε*) and dielectric loss (tan *δ*) for both microwave sintered and conventionally sintered BT and NZF ceramics samples are shown in Figures 9 and 10. For BT, it can be seen that the CV sintered pellets show the highest dielectric constant at 100 kHz. For the MW sintered BT + LiF at 1000 °C the value of *ε* is 1240, whereas for the same temperature CV sintered sample the dielectric constant value is 800 [14–16]. For all MW sintered samples it can be observed that the values of the dielectric constant are higher as compared to conventional sintered samples, this attributes to the higher density in the MW sintered specimens. The value of *ε* for all samples decreases slowly and gradually as the frequency increases from 100 to 10,000 kHz. For NZF, MW sintered pellets show the highest value of *ε* at 100 kHz. A value of 25 was obtained for NZF MW-sintered at 950 °C. It is evident that as the sintering temperature for CV methods increases from 900 °C to 1000 °C the dielectric constants decreases. As NZF is a magnetic material, the dielectric properties should be poor as shown in the results.

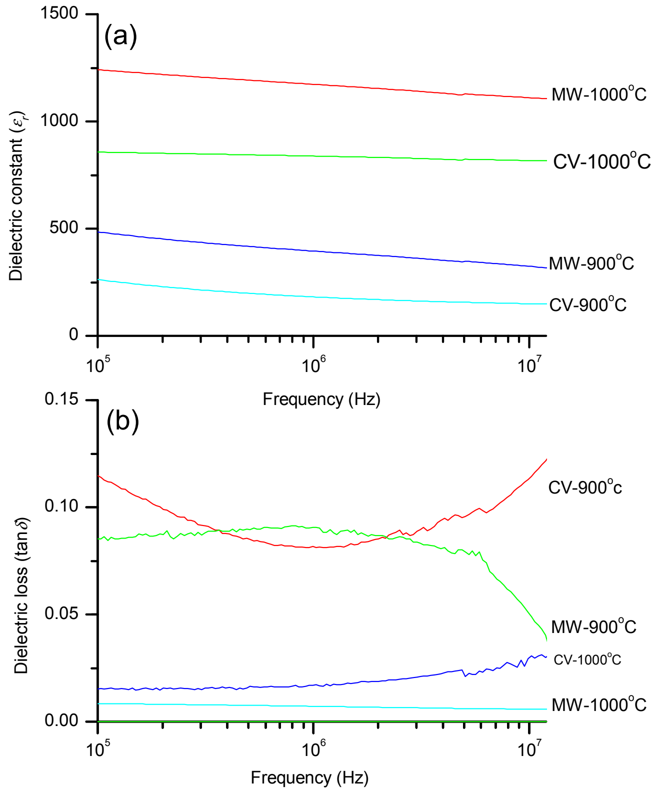

Figure 9. Frequency variation of (**a**) dielectric constant and (**b**) loss tangent of BT ceramics sintered using CV and MW techniques for 2 h and 0.5 h respectively.

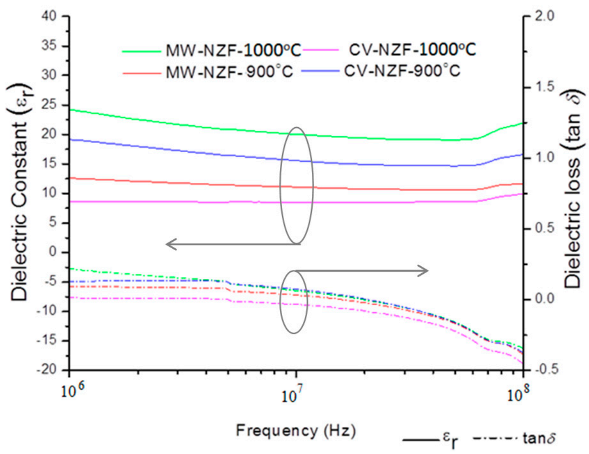

Figure 10. Frequency variation of dielectric constant and loss tangent of NZF ceramics sintered using CV and MW techniques for 2 h and 0.5 h respectively.

The room temperature P-E hysteresis loops of the BT samples sintered under various conditions are presented in Figure 11. It can be seen that the polarization of BT samples MW-sintered at 1000 °C is the highest among all the studied specimens as recorded, although all the samples show poor ferroelectric properties. It can be observed that samples sintered at low temperatures end up with a leaky nature. BT + LiF samples also exhibit a leaky nature even when sintered at 900 °C, which is attributed to the leakage from lithium itself and/or porosity.

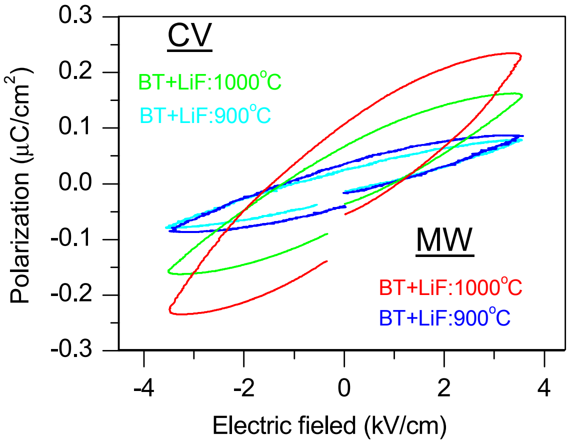

Figure 11. Room temperature P-E hysteresis loops of BT ceramics sintered using CV and MW techniques.

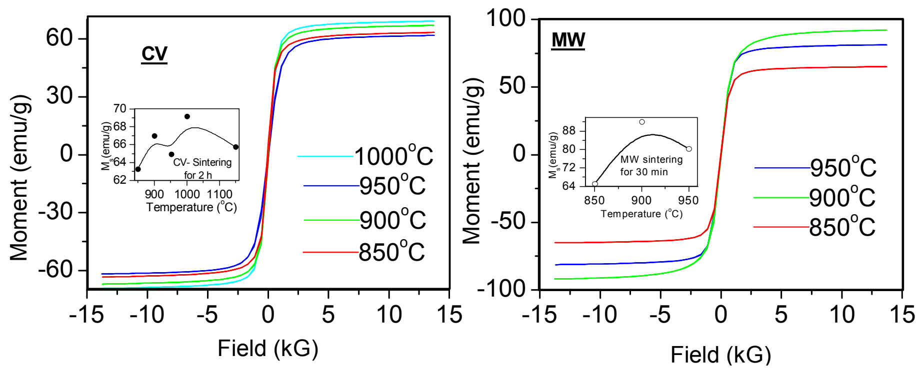

Figure 12. Room temperature M-H loops of NZF ceramics sintered using CV and MW techniques.

Figure 12 depicts the room temperature M-H loops of NZF ceramics sintered using CV and MW techniques. It can be observed that in CV sintered ceramics, the saturation magnetization (M_s) reaches its highest value of 68 emu/g at a sintering temperature of 1000 °C, whereas for MW sintered ceramics the highest value of M_s observed is 88 emu/g at a sintering temperature of 950 °C. Additionally, the M_s values for the MW sintered samples strongly correlate with the sintering temperature. This higher M_s value can be due to the 2.45 GHz MW field interacting with charged cations thus causing a change of Zn^{2+} and Fe^{3+} arrangements which are critical in the alteration of dipole moments [16,17].

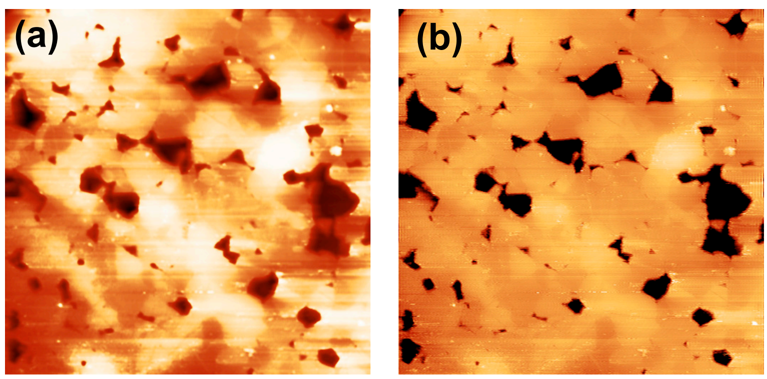

Figure 13. *Cont.*

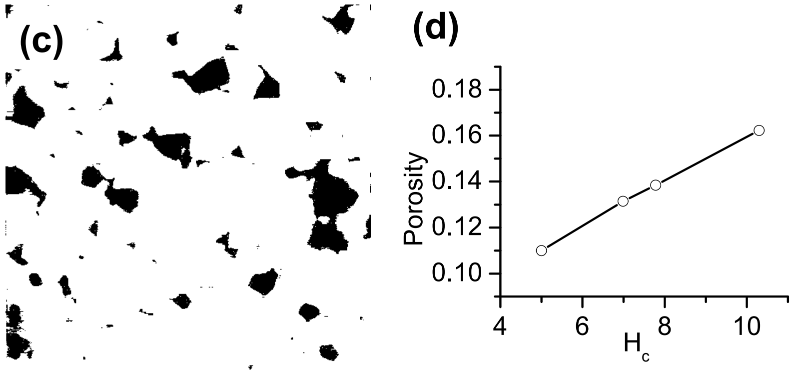

Figure 13. (**a**) Raw AFM topography, (**b**) Flattened topography (undulations removed), (**c**) Thresholding, (**d**) Porosity *vs.* magnetic coercive field.

Using AFM topography we have estimated the statistical value of porosity in the sintered ceramics. The Figure 13a–c depicts the AFM technique, which includes AFM raw topography, flattened topography (undulation removed) followed by thresholding. The percentage of voids is reflected as percentage of black pixels. Based on the estimated statistical data for NZF sintered ceramics, we have derived the relationship between the porosity and the magnetic coercive field as shown in Figure 12d. Coercive force is probably the property most sensitive to porosity and grain size. The increase in coercive force with porosity is linear, as expected. Again, this effect may be caused by the fact that the high-porosity samples contain smaller particles, which have higher coercive force.

4. Conclusions

BT and NZF ceramics were prepared using CV and MW sintering techniques and the effect of the different sintering techniques on these materials was analyzed. The grain sizes of MW sintered BT and NZF are evidently larger than conventionally sintered samples. This improvement in the structural properties influences the electrical and magnetic properties of the samples. The magnetic properties of MW sintered NZF have significantly improved. However, dielectric results show that BT with LiF samples sintered using CV process portray a leaky nature due to the presence of lithium and/or porosity due to low density, similarly that for NZF specimen sintered using CV technique exhibits low dielectric properties. Therefore, we can conclude that MW sintering methods do show that at a much shorter processing time for the same temperature it is able to achieve close to final stages of sintering compared to the sample sintered conventionally at the same temperature. In a close comparison, this information will be very much useful for the BT-NZF composite fabrication for multiferroic research purposes too. Moreover, much studied should be done for MW sintering to process BT and NZF ceramics starting using solid state reaction technique including calcination.

Acknowledgments

The authors sincerely thank Marcus Teo from the Department of Mechanical Engineering, NUS for his kind assistance in ceramics sintering and characterization.

Author Contributions

Santiranjan Shannigrahi designed the research; performed experiments; analyzed the data and wrote the paper; and Chee Kiang Ivan Tan performed the necessary experiments and contributed to the paper writing. All authors read and approved the final manuscript.

Conflicts of Interest

The authors declare no conflict of interest.

References

1. Reisel, A.D.; Schops, S.; Lenk, A.; Schmutzler, G. Microstructural comparison of conventional and microwave sintered $BaTiO_3$. *Adv. Eng. Mater*. **2007**, *9*, 400–405.
2. Sadhana, K.; Krishnaveni, T.; Praveena, K.; Bharadwaji, S.; Murthy, S.R. Microwave sintering of nanobarium titanate. *Scripta. Materialia.* **2008**, *59*, 495–498.
3. Mahboob, S.; Dutta, A.B.; Prakash, C.; Swaminathan, G.; Suryanarayana, S.V.; Prasad, G.; Kumar, G.S. Dielectric behaviour of microwave sintered rare-earth doped $BaTiO_3$ ceramics. *Mater. Sci. Eng. B* **2006**, *134*, 36–40.
4. Sun, W.; Li, J.; Liu, W.; Li, C. Preparation of fine tetragonal barium titanate powder by a microwave-hydrothermal process. *J. Am. Ceram. Soc.* **2006**, *89*, 118–123.
5. Yodoji, P.; Peelamedu, R.; Agrawal, D.; Roy, R. Microwave sintering of Ni-Zn ferrites: Comparison with conventional sintering. *Mater. Sci. Eng. B* **2003**, *98*, 269–278.
6. Ghasemi, A.; Mousavinia, M. Structural and magnetic evaluation of substituted $NiZnFe_2O_4$ particles synthesized by conventional sol-gel method. *Cerm. Int.* **2014**, in press.
7. Shannigrahi, S.R.; Pramoda, K.P.; Nugroho, F.A.A. Synthesis and characterization of microwave sintered ferrite powders and their composite films for practical applications. *J. Mag. Mag. Mater*. **2012**, *324*, 140–145.
8. Pallathadka, K.P.; Huang, A.; Shannigrahi, S.R. On some properties of PZT–NZF composite films manufactured by hybrid synthesis route. *Ceram. Int.* **2011**, *37*, 431–435
9. Sorescu, M.; Diamandescu, L.; Peelamedu, R., Roy, R.; Yadoji, P. Structural and magnetic properties of NiZn ferrites prepared by microwave sintering. *J. Magn. Magn. Mater.* **2004**, *279*, 195–201.
10. Peelamedu, R.; Grimes, C.; Agrawal, D.; Roy, R. Ultralow dielectric constant nickel-zinc ferrites using microwave sintering. *J. Mater. Res.* **2003**, *18*, 2292–2295.
11. Walker, B.E.; Rice, J.R.W.; PohankaR, C.; Spann, J.R. Densification and strength of $BaTiO_3$, with LiF and MgO additives. *Am. Cemm. Soc. Bull.* **1976**, *55*, 284–285.
12. Zadeh, H.N.; Glitzky, C.; Dorfel, I.; Rab, T. Low temperature sintering of barium titanate ceramics assisted by addition of lithium fluoride-containing sintering additives. *J. Eu. Ceram. Soc*. **2009**, *30*, 81–86.
13. Lange, F.F. Liquid phase sintering: Are liquids squeezed out from between compressed particles? *J. Am. Ceram. Soc.* **1982**, *65*, C23.

14. Hsiang, H.I.; His, C.S.; Huang, C.C.; Fu, S.L. Sintering behavior and dielectric properties of $BaTiO_3$ ceramics with glass addition for internal capacitor of LTCC. *J. Alloys Comp*. **2008**, *459*, 307–310.
15. Gao, L.; Huang, Y.; Hu, Y.; Du, H. Dielectric and ferroelectric properties of (1-x) $BaTiO_3$-$xBi_{0.5}Na_{0.5}TiO_3$ ceramics. *Ceram. Int*. **2007**, *33*, 1041–1046.
16. Gao, S.; Wu, S.; Zhang, Y.; Yang, H.; Wang, X. Study on the microstructure and dielectric properties of X9R ceramics based on $BaTiO_3$. *Mater. Sci. Eng. B* **2011**, *176*, 68–71.
17. Thostenson, E.T.; Chou, T.W. Microwave processing: Fundamentals and applications. *Composites Part. A* **1999**, *30*, 1055–1071.